



HAL
open science

Preadipocyte conversion to macrophage. Evidence of plasticity

Guillaume Charrière, Béatrice Cousin, Emmanuelle Arnaud, Mireille André,
Francis Bacou, Luc Pénicaud, Louis Casteilla

► **To cite this version:**

Guillaume Charrière, Béatrice Cousin, Emmanuelle Arnaud, Mireille André, Francis Bacou, et al.. Preadipocyte conversion to macrophage. Evidence of plasticity. *Journal of Biological Chemistry*, 2003, 278 (11), pp.9850-9855. 10.1074/jbc.M210811200 . hal-02678883

HAL Id: hal-02678883

<https://hal.inrae.fr/hal-02678883>

Submitted on 31 May 2020

HAL is a multi-disciplinary open access archive for the deposit and dissemination of scientific research documents, whether they are published or not. The documents may come from teaching and research institutions in France or abroad, or from public or private research centers.

L'archive ouverte pluridisciplinaire **HAL**, est destinée au dépôt et à la diffusion de documents scientifiques de niveau recherche, publiés ou non, émanant des établissements d'enseignement et de recherche français ou étrangers, des laboratoires publics ou privés.

Preadipocyte Conversion to Macrophage

EVIDENCE OF PLASTICITY*

Received for publication, October 23, 2002, and in revised form, December 10, 2002
Published, JBC Papers in Press, January 7, 2003, DOI 10.1074/jbc.M210811200

Guillaume Charrière‡§, Béatrice Cousin‡, Emmanuelle Arnaud‡, Mireille André‡,
Francis Bacou¶, Luc Pénicaud‡, and Louis Casteilla‡¶

From the ‡Unité Mixte de Recherche 5018 Université Paul Sabatier CNRS, IFR31, Bat L1, Centre Hospitalier
Universitaire Rangueil, 31403 Toulouse, France and the ¶Unité Mixte de Recherche 866 Différenciation Cellulaire et
Croissance, INRA, 34060 Montpellier Cedex 01, France

Preadipocytes are present throughout adult life in adipose tissues and can proliferate and differentiate into mature adipocytes according to the energy balance. An increasing number of reports demonstrate that cells from adipose lineages (preadipocytes and adipocytes) and macrophages share numerous functional or antigenic properties. No large scale comparison reflecting the phenotype complexity has been performed between these different cell types until now. We used profiling analysis to define the common features shared by preadipocyte, adipocyte, and macrophage populations. Our analysis showed that the preadipocyte profile is surprisingly closer to the macrophage than to the adipocyte profile. From these data, we hypothesized that in a macrophage environment preadipocytes could effectively be converted into macrophages. We injected labeled stroma-vascular cells isolated from mouse white adipose tissue or 3T3-L1 preadipocyte cell line into the peritoneal cavity of nude mice and investigated changes in their phenotype. Preadipocytes rapidly and massively acquired high phagocytic activity and index. 60–70% of preadipocytes also expressed five macrophage-specific antigens: F4/80, Mac-1, CD80, CD86, and CD45. These values were similar to those observed for peritoneal macrophages. *In vitro* experiments showed that cell-to-cell contact between preadipocytes and peritoneal macrophages partially induced this preadipocyte phenotype conversion. Overall, these results suggest that preadipocyte and macrophage phenotypes are very similar and that preadipocytes have the potential to be very efficiently and rapidly converted into macrophages. This work emphasizes the great cellular plasticity of adipose precursors and reinforces the link between adipose tissue and innate immunity processes.

White adipose tissue is known to undergo considerable changes. It develops mainly after birth, and its mass increases greatly in obesity (1). Conversely, it almost completely disappears during starvation or cachexia (2). Tissue growth is due to increase in size and/or number of mature adipocytes. These mature cells differentiate from progenitors, *i.e.* preadipocytes,

which are present in stroma-vascular fraction (SVF)¹ and can be recruited throughout adult life (3). This phenomenon seems to be reversible, and several reports describe the dedifferentiation of mature adipocytes into a preadipocyte state (4–6).

Analysis of the literature revealed that adipocyte and monocyte/macrophage lineages have many features in common (3, 7–14). In particular, proteins or functions known to be specific to one lineage are characterized in the other. For instance, mature adipose cells express a membrane-bound NADPH oxidase similar to that present in specialized phagocytes (8), and preadipocytes and adipocytes secrete numerous inflammatory cytokines such as tumor necrosis factor α and are sensitive to lipopolysaccharide activation (14). Conversely, aP2 and peroxisome proliferator-activated receptor γ , long described as specific to adipocyte lineage, have been detected in macrophages (12).

Recently, we reported that preadipocytes of the 3T3-L1 cell line as well as preadipocytes in primary culture display phagocytic and microbicidal activities similar to those of specialized phagocytic cells, *i.e.* macrophages (15). This activity is lower than that of macrophages but is stimulated in inflammatory situations (16). A putative link between adipose and macrophage lineages was strengthened by the detection on preadipocytes and adipocytes of MOMA-2 antigen, a marker of monocyte-macrophage lineage (15). However, the most commonly used macrophage cell surface markers, F4/80 or Mac-1 (CD11b) (17), were not detected under standard conditions on preadipocytes or adipocytes.

Despite all these common features, no systematic or large scale comparison between these two lineages has been performed to further analyze the similarities among preadipocyte, adipocyte, and macrophage phenotypes. This can be done by large scale gene expression data set analysis such as transcriptome profiling. This technique is the commonest and most powerful tool to identify genes of interest differentially expressed according to time scale and/or treatment (18, 19). However, it has rarely been used to characterize and compare different phenotypes (20, 21).

We used this technique to compare adipocyte and macrophage lineages and found close similarities between preadipocyte and macrophage phenotypes, suggesting that preadipocytes can convert to macrophages. To test this hypothesis *in vivo*, we chose the peritoneal cavity as an adequate environment to support macrophage phenotype after preadipocyte transplantation. We were able to demonstrate that preadipocytes can efficiently and rapidly convert into macrophages.

* This work was supported by Grant 4CS01F from Génopôle Toulouse and Association Française contre les Myopathies/INSERM. The costs of publication of this article were defrayed in part by the payment of page charges. This article must therefore be hereby marked "advertisement" in accordance with 18 U.S.C. Section 1734 solely to indicate this fact.

§ Recipient of a fellowship from the Ministry of National Education, Research and Technology.

¶ To whom correspondence should be addressed. Tel.: 33-5-62-17-08-91; Fax: 33-5-62-17-09-05; E-mail: casteil@toulouse.inserm.fr.

¹ The abbreviations used are: SVF, stroma-vascular fraction; DAPI, 4',6'-diamidino-2-phenylindole; PBS, phosphate-buffered saline; DMEM, Dulbecco's modified Eagle's medium; NCS, newborn calf serum; GFP, green fluorescent protein; CMV, cytomegalovirus; FITC, fluorescein isothiocyanate.

EXPERIMENTAL PROCEDURES

Reagents and Cell Lines—All components for cell culture were purchased from Invitrogen. The fluorescent nuclear marker 4',6-diamidino-2-phenylindole (DAPI) was purchased from Sigma Aldrich Chimie. Adenovirus CMV-GFP was a gift from Prof. P. Moullier, Laboratoire de Thérapie Génique, AFM, Nantes, France. Antibodies: anti-F4/80 was obtained from Serotec (Cergy Saint-Christophe, France), and all others were obtained from Clinisciences (Mont-Rouge, France). Immunochemical reagents were purchased from Dako (Trappes, France). Collagenase (Roche Diagnostics) was purchased from Roche Molecular Biochemicals (Meylan, France). Ob17 and Hgfu cell lines were kindly provided by Dr. Dani, Nice, France. J774.2 and RAW 264.7 cell lines were purchased from ECACC.

Animals and Cell Culture—5–6-week-old Swiss nu/nu and C57B6J mice (Harlan, France) were housed in microisolator cages in conventional animal quarters. All animals had free access to food and water and were sacrificed with CO₂.

Peritoneal cells were obtained by washing the peritoneal cavity of mice with 5 ml of sterile PBS and grown in DMEM/F12 containing 10% heat-inactivated newborn calf serum (NCS). SVF and mature adipocytes were obtained from inguinal fat depot as previously described (22). Briefly, adipose tissue was digested with 2 mg/ml collagenase in 2% albumin-containing DMEM/F12 medium for 30 min at 37 °C. After filtration through a 25- μ m nylon membrane to eliminate undigested fragments, cells were centrifuged at 600 \times g for 10 min to separate mature adipocytes from pellets of SVF cells. SVF cells were counted (Coulter Z2) and plated (30,000 cells/cm²) in DMEM/F12 10% NCS medium. Six hours after plating, cells were washed to remove all non-adherent cells.

All cell lines were maintained before confluence in DMEM containing 10% heat-inactivated fetal calf serum and glutamine (2 mM). 3T3-F442A adipose differentiation was performed by adding rosiglitazone (100 nM) at the first confluence day, and then cells were fed every 2 days with the same medium. 3T3-F442A-differentiated cells were stopped 7 days after the beginning of differentiation.

Preadipocyte Labeling and Implantation in the Peritoneal Cavity of Nude Mice—Culture medium containing 1 μ g/ml DAPI or 70 plaque-forming units/cell adenovirus containing green fluorescent protein (GFP) cDNA under the control of cytomegalovirus (CMV) promoter was added for 12 h on SVF cells (6 h after plating) or on non-confluent 3T3-L1 cells. Adequate adenovirus titer was determined after dose response infection study. This concentration was chosen to achieve significant labeling with limited toxic effects. The cells were then rinsed five times with DMEM + 10% fetal calf serum or DMEM/F12 + 10% NCS and twice with PBS. After trypsinization, preadipocytes were collected and washed twice with PBS. Before injection in the peritoneal cavity, cells were resuspended in PBS (2 \times 10⁶ in 500 μ l). For control experiments, the supernatant of the last wash was collected and filtered at 0.2 μ m before injection (500 μ l).

Preadipocyte and Macrophage Co-culture Experiments—Co-cultures were performed in DMEM/F12 + 10% NCS for 24 h. 3T3-L1 preadipocytes were labeled and washed as for *in vivo* experiments. Labeled preadipocytes and non-labeled peritoneal macrophages were plated (12,500 3T3-L1/cm² and 25,000 macrophages/cm²) together onto glass slides (Lab-tek slides, Nalge Nunc International, Naperville, IL) or in two chambers separated by a track-etched membrane (pore size, 0.4 μ m).

Measurement of Phagocytic Activity and Phagocytic Index—Yeast (*Candida parapsilosis*) was washed in PBS and suspended at 4 \times 10⁷ yeast/ml in DMEM/F12 + 4% NCS without antibiotics (23). After culture for 24 h on Lab-tek slides, peritoneal cells were incubated 45 min in 1 ml of yeast suspension at 37 °C in a CO₂ chamber. Slides were then washed three times with PBS and mounted with fluorescent mounting medium. Mounted Lab-tek slides were observed with phased and UV lights (UV filter: λ_e , 340–380 nm; λ_a , 425 nm) or FITC (FITC filter: λ_e , 450–490 nm; λ_a , 515 nm). Phagocytic activity is the percentage of phagocytizing cells, and the phagocytic index is the average number of engulfed yeast per phagocytizing cell.

Immunocytochemistry Experiments—For immunocytochemistry experiments, 3T3-L1 or peritoneal cells were cytospun onto glass slides and fixed in PBS with 3.7% paraformaldehyde for 30 min. Standard methodology was used to detect immunological staining (15). PBS containing 0.01% polyoxyethylenesorbitant-monolaurate (Tween 20) or 1% fatty acid free bovine serum albumin was used in DAPI-labeled or GFP-expressing cell experiments respectively. Primary antibodies (IgG₂, rat anti-mouse) concentrations were 100 μ g/ml for anti-Mac-1, 50 μ g/ml for anti-F4/80, and anti-CD86, 500 μ g/ml for anti-CD80, and 25

μ g/ml for anti-MHCII. A non-relevant IgG₂ isotype antibody was used as negative control. The secondary antibody was a rabbit anti-rat immunoglobulin (Fab' fragment) coupled with rhodamin-phycoerythrin (RPE) (concentration 5 μ g/ml). RPE was visualized with fluorescent light (TX2 filter: λ_e , 560/40 nm; λ_a , 645/75 nm).

mRNA Extraction—RNA was isolated from cell culture, isolated cells, or cold powdered tissue samples using Tripur reagent (Roche Molecular Biochemicals) according to the manufacturer's instructions. Total RNA was treated for 30 min at 37 °C with DNase to eliminate potential DNA residues. RNA was then purified using the phenol/chloroform extraction procedure (24). RNA quality was checked by agarose gel electrophoresis and spectrophotometric analysis (OD_{260/280}).

Probe Preparation and cDNA Microarray Hybridization—Ten micrograms of total RNA (denatured at 70 °C for 10 min) were reverse-transcribed for 2 h at 42 °C with 1 μ l (200 units) of Superscript II reverse transcriptase (Invitrogen), 4 μ g of 25 mer/oligo(dT), 80 μ Ci of [α -³³P]dCTP (10 mCi/ml, 2500 mCi/mmol, Amersham Biosciences), 1 mM each of dATP, dGTP, dTTP, 3.3 mM dithiothreitol, 2 μ l of H₂O, and 6 μ l of 5 \times first-strand buffer (Invitrogen) in a final volume of 30 μ l. After 1 h, 1 μ l of Superscript II reverse transcriptase was added to the reaction mixture. The resulting [³³P]cDNA probes were purified with ProbeQuant G-50 Micro columns (Amersham Biosciences) following the manufacturer's instructions. After counting, probes with a total activity higher than 2 \times 10⁷ cpm were the only ones to be hybridized. Mouse GeneFilters (GF400 from ResGen, Invitrogen) were used for profiling expression analysis. GeneFilters contain 5185 genes (75% are expressed sequence tags (ESTs)). The membranes were pretreated with boiled 0.5% SDS for 10 min. Prehybridization was performed for 4 h at 42 °C in MicroHyb hybridization solution (ResGen) with 5 μ g of denatured mouse Cot-1 and 4 μ g of poly(dA) as blocking reagents. The column-purified and denatured probes were then added and hybridized at 42 °C for 16 h. After hybridization, the membranes were successively washed twice for 10 min at 50 °C in roller tubes containing 2 \times standard saline citrate solution (SSC) and 1% SDS. The last two washes were carried out in a plastic box with horizontal shaking: 2 \times SSC and 1% SDS for 20 min at 50 °C and 0.5 \times SSC and 1% SDS for 15 min at 55 °C. The membranes were then exposed to low energy phosphorimage screens for 2 days. Images were acquired using PhosphorImager 445 SI (Molecular Dynamics, Amersham Biosciences, Sunnyvale, CA), and analyzed with IMAGENE 4.0 (Biodiscovery, Marina del Rey) and Excel (Microsoft) software. Each hybridization was performed with independent RNA samples (cell preparation and RNA extraction).

Microarray Data Analysis—For each hybridization, the mean of local background incremented with two S.D. was subtracted from each spot's intensity. After this correction, all positive values were considered as significant and transformed into log₁₀ values. Hybridizations were then normalized by dividing the intensity of each spot by the mean of the control spot intensity of total genomic DNA (Tg) spotted by the manufacturer onto membrane. Profile analyses were performed using J-Express 2.0 software (Molmine, Ref. 25) and ExpressionSieve™ 1.0 lite (BioSieve). "Random" profile was created using the RAND Excel function (Microsoft).

Statistical Analysis—Results are expressed as means \pm S.E. The statistical significance of differences between means was evaluated using the unpaired Student's *t* test. In the time course experiments, statistical significance was evaluated using one-way ANOVA analysis.

RESULTS

Microarray Analysis—All RNA samples were purified from murine cells to avoid mismatch recognition between the labeled probe derived from these samples and the mouse cDNA spotted onto matrix. To obtain the best physiological relevance, we used several cell lines for one phenotype as well as cells freshly isolated from mouse tissues. However, for one phenotype, data from immortalized or non-immortalized cells were individualized. 3T3-L1, 3T3-F442A, Ob17, Hgfu preadipocyte, and RAW 264.7, J774.2 murine cell lines were the most often used to investigate adipocyte and macrophage properties, respectively. Preadipocytes were enriched from SVF cells by plating and culturing for 48 h. To exclude the possibility of contaminating macrophages, we tested for F4/80 or Mac-1-positive cells. Less than 1% of SVF cells were expressing these antigens (data not shown). The independent hybridizations corresponding to each phenotype class were gathered together to build height representative profiles, named metaprofiles (Table I). To build them,

TABLE I
Experimental design of metaprofiles

Phenotype	Preadipocyte		Adipocyte		Macrophage		Liver
Metaprofile	Preadipocyte line	SVF	Adipocyte line	Adipocyte	Macrophage line	Peritoneal macrophage	Liver
Hybridizations	3T3-L1 3T3-F442A Ob17 Hgfu	SVF cells in primary culture	Differentiated 3T3-F442A	Isolated adipocytes	RAW 264.7 J774.2	Peritoneal exudated cells	Tissue samples

genes were first filtered to retain only those whom expression was detected in more than 50% of hybridizations. The mean of their positive hybridization values were calculated and retained. The resulting dataset was again filtered to normalize the number of positive genes and to exclude genes that were always negative (2040 of 5185 initial genes) or positive (133) in all metaprofiles.

At this stage and to test the significance of clustering, we included a “random” metaprofile in the dataset. In this metaprofile, the values of hybridizations were distributed at random. The resulting dataset contained 468 genes. Before clustering, column variances were normalized (J-Express, Plug-ins).

Interpretation of Metaprofiles with a Hierarchical Classification Algorithm—The metaprofiles in the dataset were clustered with a hierarchical classification algorithm based on Pearson’s correlation distance ($d = 1 - r$) and average linkage. The clustering algorithm separated metaprofiles into two distinct clusters (Fig. 1). The first cluster included liver and random metaprofiles. As expected, the two negative controls random and liver metaprofiles were the most isolated profiles with a low similarity between them ($d > 0.8$). The second cluster contained all cellular metaprofiles. Thus, the macrophage phenotypes, which corresponded to a differentiated phenotype, were closer to the preadipocyte metaprofiles ($d \leq 0.5$) than to the metaprofiles of differentiated adipocytes (from fatty tissue or also preadipocyte cell lines) ($d > 0.5$). Within the subcluster, preadipocyte or macrophage metaprofiles were systematically paired according to the nature of the sample (immortalized cell lines *versus* non-immortalized cells). This common behavior suggested a strong similarity between the two phenotypes, although the identification of gene clusters preferentially expressed in one metaprofile demonstrated that they were not identical. However, because of this close resemblance, the question of putative conversion of preadipocytes into macrophages emerged from this analysis. To address this question, we decided to transplant labeled preadipocytes into an environment suitable for supporting the macrophage phenotype (*i.e.* the peritoneal cavity).

Phenotype of DAPI-positive (DAPI⁺) SVF Cells after Peritoneal Injection—Preadipocytes were labeled with DAPI before injection into the peritoneal cavity. Two controls were performed to demonstrate the absence of staining of endogenous peritoneal cells by contaminating DAPI during injection of DAPI-labeled cells. First, supernatants of labeling washings and highly concentrated DAPI solution (500 μ l) were directly injected into the peritoneal cavity. Second, DAPI-labeled preadipocytes and non-labeled peritoneal macrophages were cocultured for 2 days in 2 chambers separated by a track-etched membrane (pore size, 0.4 μ m). No contaminating staining was observed at any time in either case. Furthermore, we checked that DAPI had no effect on the preadipocyte phenotype, its proliferation and differentiation process in our conditions (data not shown).

Before injection, $28 \pm 4\%$ of SVF cells were phagocytizing with a phagocytic index of 6 ± 1 and less than 1% were expressing the mature macrophage antigens F4/80 or Mac-1. Twenty-four hours after their injection into the peritoneal cav-

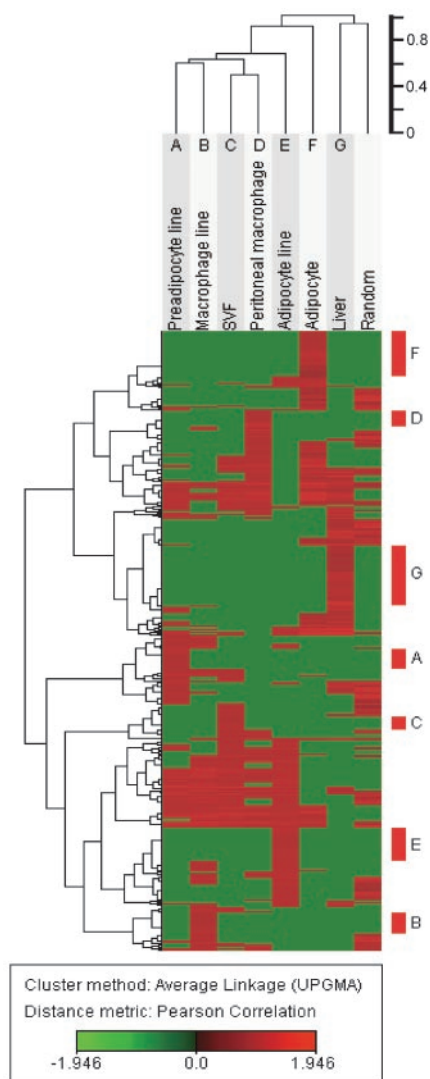


FIG. 1. **Metaprofile comparison with hierarchical clustering algorithm.** Metaprofiles are ordered along the x-axis, and genes are ordered along the y-axis. Trees represent the proportional distance measured between each metaprofile (*top*) or each gene (*left*). Metaprofile-specific gene clusters are identified by red bars and their corresponding letters (*right*). Letters are shown at the *top* of their corresponding metaprofile.

ity, $15 \pm 2\%$ of peritoneal cells were DAPI⁺, and the phagocytic activity of these cells reached $92 \pm 1\%$ with a phagocytic index of 18 ± 3 . Similar results were obtained 6 days after injection (Fig. 2, A and B). The time course of these changes was investigated. As soon as 24 h after cell transplantation, $61 \pm 1\%$ and $81 \pm 3\%$ of DAPI⁺ cells were strongly stained with antibodies against F4/80 and Mac-1 respectively (Fig. 2, C and D). All values were significantly higher ($p < 0.01$) than those measured on non-injected SVF cells and were not significantly different from those of peritoneal macrophages ($98 \pm 1\%$ of macrophages presented phagocytic activity with a phagocytic index of 19 ± 1 ; $63 \pm 7\%$ and $70 \pm 4\%$ were F4/80⁺ and Mac-1⁺,

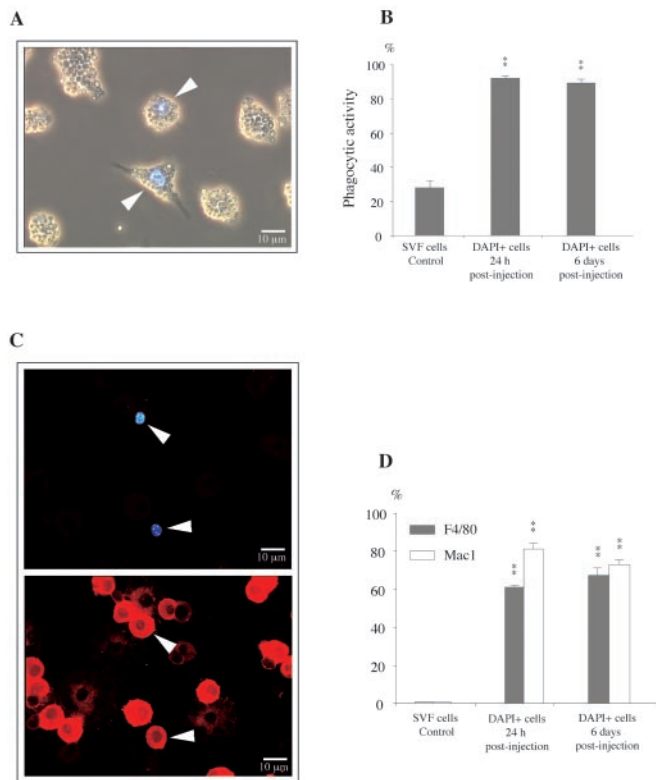


FIG. 2. Phagocytic activity and antigenic features of DAPI-labeled SVF cells after peritoneal injection. *A*, phagocytosis of peritoneal cells 24 h after peritoneal injection of DAPI-labeled SVF cells. Contrast phase light and UV filter were used. Blue nuclei correspond to cells stained by DAPI. Closed arrowhead, phagocytizing DAPI⁺ cells. *B*, the phagocytic activity of DAPI⁺ SVF cells was measured 24 h or 6 days after peritoneal injection. Phagocytic activity represents the percentage of DAPI⁺ phagocytizing cells per total DAPI⁺ cells. Results are means \pm S.E. of at least three independent experiments. All results differed significantly (**, $p < 0.01$) from values obtained with SVF cells before the injection. *C*, immunocytochemistry was performed 24 h after peritoneal injection of labeled cells with anti-F4/80 antibody. The secondary antibody was coupled to RPE. UV filter (top), TX2 filter (bottom). Closed arrowhead, DAPI⁺ F4/80⁺ cells; *D*, the percentages of F4/80⁺ and Mac-1⁺ cells per total DAPI⁺ cells were measured 24 h and 6 days after peritoneal injection of DAPI-labeled cells. Results are means \pm S.E. of at least three independent experiments. All results differed significantly (**, $p < 0.01$) from values obtained with SVF cells before injection.

respectively). Afterward, these values remained at this level whatever the time of sampling.

Time Course of Phenotype Changes of Labeled 3T3-L1 Cells after Injection into the Peritoneal Cavity—To determine whether a clonal preadipocyte population had similar behavior, immortalized 3T3-L1 preadipocytes were used. In basal conditions, the phagocytic activity and index of 3T3-L1 were $26 \pm 5\%$ and 3 ± 1 yeast/cell, respectively (see below). None of these cells expressed F4/80 or Mac-1 (data not shown). Six hours after injection, $23 \pm 2\%$ of peritoneal cells were DAPI⁺. Phagocytic activity and index of these cells dramatically increased and reached $81 \pm 6\%$ and 15 ± 1 respectively (Fig. 3A). $72 \pm 3\%$ of DAPI⁺ cells expressed F4/80, and similar values were observed for Mac-1 expression (Fig. 3B). No further significant change of these parameters was observed whatever the time of sampling (Fig. 3, A and B). All values were significantly higher ($p < 0.01$) than those observed in basal conditions and were not significantly different from those of peritoneal macrophages. The expression of CD80, CD86, and MHCII was then investigated. CD80, CD86, and MHCII antibodies stained $62 \pm 4\%$, $63 \pm 5\%$, and $20.1 \pm 0.1\%$ of peritoneal cells respectively (Fig. 3C). No staining with any antibodies was detected in preadi-

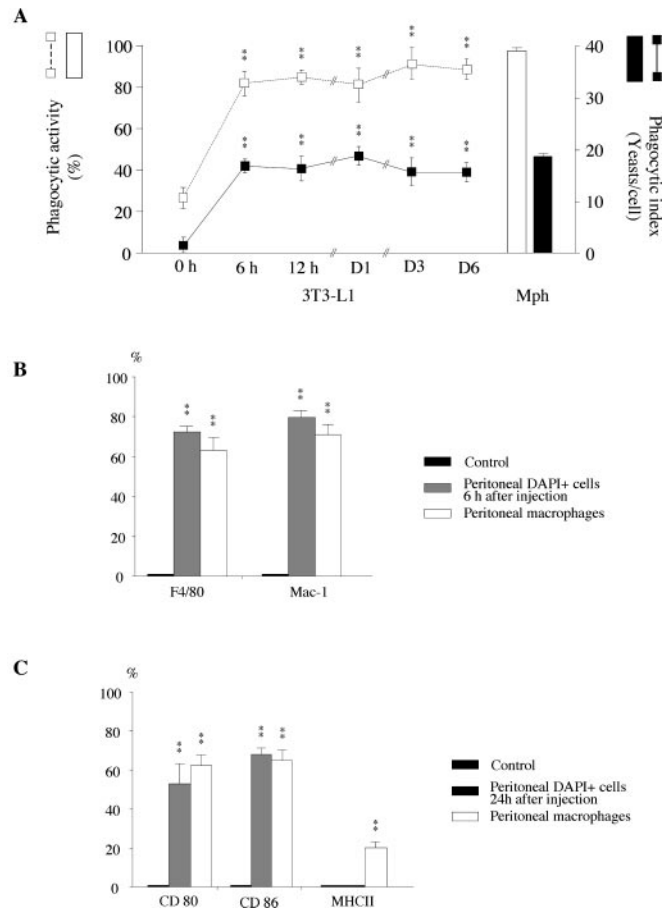


FIG. 3. Phenotype modifications of DAPI-labeled 3T3-L1 cells after peritoneal injection. *A*, time course of phagocytic activity and index of DAPI⁺ 3T3-L1 cells. Phagocytic activity represents the percentage of phagocytizing cells per total DAPI⁺ cells (broken line, left y axis). Phagocytic index represents the average number of engulfed yeast per phagocytic cell (continuous line, right y axis). Results are means \pm S.E. of at least three independent experiments. All results differed significantly (**, $p < 0.01$) from values obtained with non-confluent 3T3-L1 cells. Peritoneal macrophages were used as positive controls. *B*, expression of macrophage-specific markers by peritoneal DAPI⁺ cells. Six hours after the peritoneal injection of labeled cells, immunocytochemistry experiments were performed with primary antibodies and RPE-coupled secondary antibody. Values represent the percentage of F4/80⁺ and Mac-1⁺ cells per total DAPI⁺ cells. Results are means \pm S.E. of at least three independent experiments. All results differed significantly (**, $p < 0.01$) from values obtained with non-confluent 3T3-L1 controls. *C*, additional characterization of peritoneal DAPI⁺ cells. Twenty-four hours after peritoneal injection of labeled cells, immunocytochemistry experiments were performed with primary antibodies anti-CD80, anti-CD86, and anti-MHCII. Values represent the percentage of positive cells per total DAPI⁺ cells. Results are means \pm S.E. of at least three independent experiments. The means differed significantly (**, $p < 0.01$) from values obtained with non-confluent 3T3-L1 controls.

pocytes before injection. Twenty-four hours after peritoneal injection of 3T3-L1 cells, $53 \pm 10\%$ and $68 \pm 3\%$ of DAPI⁺ cells expressed CD80 and CD86 respectively (Fig. 3C). The values obtained with CD80 and CD86 were not significantly different from those of peritoneal cells. Similar results were obtained with CD45 antigen, which is considered as pan-hematopoietic (data not shown). Under the same conditions, MHCII was never detected on 3T3L1 DAPI⁺ cells (Fig. 3C) as well as on primary adipocyte precursors (data not shown).

To confirm these results with other labeling techniques, similar transplantation experiments were performed with 3T3-L1 after adenovirus-mediated overexpression of GFP (GFP⁺). After overnight infection with 70 plaque-forming units/cell of the

CMV-GFP adenovirus, 70% of the cultured 3T3-L1 cells expressed GFP. The absence of free viral particles in the injection medium was checked by injection of adenovirus-infected 3T3-L1 supernatant into the peritoneal cavity. No GFP⁺ peritoneal cells were observed 1 day after supernatant injection.

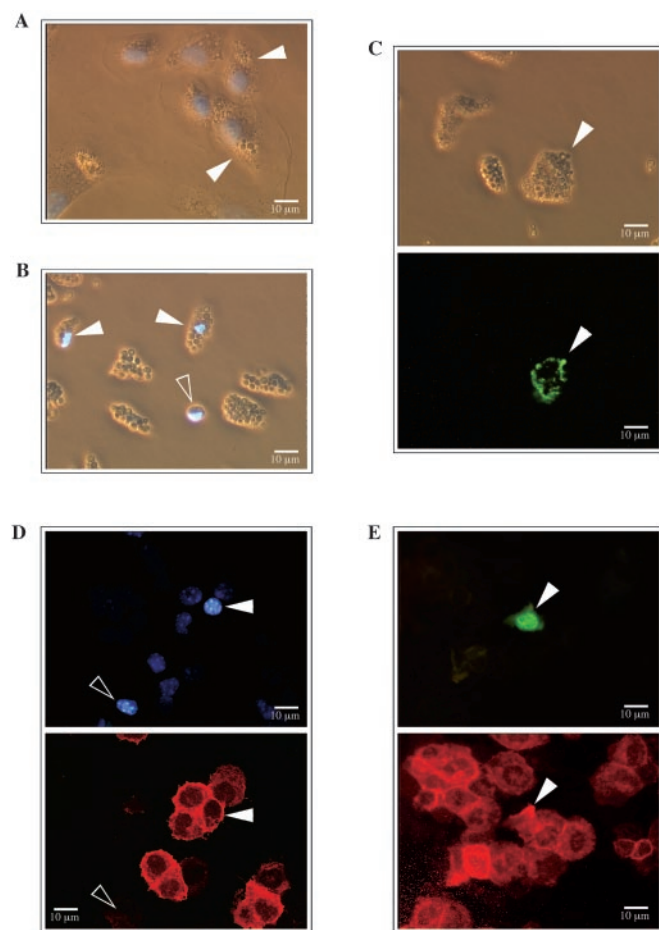


FIG. 4. 3T3-L1 phenotype before and after peritoneal injection. A, phagocytosis of DAPI-labeled 3T3-L1 cells under standard conditions. B, phagocytosis of peritoneal cells 6 days after peritoneal injection of DAPI-labeled 3T3-L1 cells. Contrast phase light and UV filter were used. Blue nuclei correspond to cells stained by DAPI. Closed arrowhead, DAPI⁺ phagocytizing cells, open arrowhead, DAPI⁺ non-phagocytizing cells. C, phagocytosis of peritoneal cells 24 h after peritoneal injection of GFP-expressing 3T3-L1. Contrast phase light (top) and FITC filter (bottom). Closed arrowhead, GFP⁺ phagocytizing cell. D, immunocytochemistry was performed 24 h after peritoneal injection of DAPI-labeled 3T3-L1 with anti-F4/80 antibody. The secondary antibody was coupled to RPE. DAPI staining (blue light, top), RPE fluorescence (red light, bottom). Closed arrowhead, DAPI⁺ F4/80⁺ cells; open arrowhead, DAPI⁺ F4/80⁻ cells. E, immunocytochemistry was performed 24 h after peritoneal injection of GFP expressing 3T3-L1 with anti-F4/80 antibody. The secondary antibody was coupled to RPE. GFP expression (green light, top), RPE fluorescence (red light, bottom). Closed arrowhead, GFP⁺ F4/80⁺ cells.

One day after peritoneal injection, the changes in GFP⁺ cells were similar to those observed in DAPI⁺ cells (Fig. 4). These observations confirmed the results obtained with the DAPI-labeled cells.

Effect of Co-cultured Macrophages on 3T3-L1 Phenotype—DAPI⁺ or GFP⁺ 3T3-L1 cells were co-cultured with peritoneal macrophages either together on Lab-tek slides or in two chambers separated by a track-etched membrane. After 1 day in co-culture without separation membrane, phagocytic activity of the stained preadipocytes significantly increased and reached $45 \pm 5\%$ (Table II). In addition, after co-culture with peritoneal macrophages, F4/80 and Mac-1 positive preadipocytes were detected ($8.3 \pm 0.3\%$ and $9 \pm 1\%$ of DAPI⁺ cells (Table II). When preadipocytes were co-cultured with C2C12 myoblasts, no change of the preadipocyte phenotype was noted. When preadipocytes were co-cultured without cell-to-cell contact, in the 2-chamber system, no change in phagocytic activity or expression of macrophage antigens was observed (Table II).

DISCUSSION

To test the similarity between cells of adipocyte lineage (*i.e.* preadipocytes and adipocytes) and macrophages without focusing on specific genes, we decided to use the transcriptome profiling approach. First, differences highlighted by our analysis between immortalized and non-immortalized cells, whatever their phenotype, confirmed the previous report and *a posteriori* our approach (18).

The result of profiling is unambiguous. Indeed, macrophages are genomically closer to adipocyte precursors than to adipocytes. The link between a differentiated phenotype, *i.e.* macrophage, and proliferating precursor cells excluded any artifactual clustering due to proliferating potential. This closeness is true for phenotypes derived from cell lines as well as those derived from cells purified from mice. This argues for close resemblance between preadipocytes and macrophages even though each metaprofile can be identified by specific gene clusters under standard conditions. This conclusion is consistent with our previous work (15). The strong proximity of preadipocyte and macrophage phenotypes raises the question of whether preadipocytes have the potential to transdifferentiate into macrophages. To test this hypothesis, we chose to graft preadipocytes into a site that is suitable for supporting the macrophage phenotype, *i.e.* the peritoneal cavity.

Recent implantation studies have used the fluorescent nuclear marker DAPI to trace implanted cells (26, 27). DAPI, which binds strongly to adenine-thymidine-rich sites in nuclear DNA, is easy to use with all cell types whatever their proliferation state, and labels 100% of treated cells. These characteristics are very convenient for labeling cells in primary culture, which are often refractory to transfection or infection. An alternative would be to use adenovirus. Adenovirus has been extensively used to transiently express protein in infected cells (28), but it is not as effective as DAPI, especially for preadipocyte cell lines and SVF, and leads *in vivo* to inflammatory

TABLE II

Macrophage contact is necessary for specific conversion of preadipocytes into macrophages

Preadipocytes and macrophages were co-cultured together or separated by a track-etched membrane. After 24 h, phagocytic activity was measured and the number of F4/80⁺ or Mac-1⁺ cells was counted. Values represent the percentage of phagocytic cells or F4/80⁺ or Mac-1⁺ cells in the total number of DAPI⁺ cells. Results are means \pm S.E. of at least three independent experiments. *, $p < 0.05$ and **, $p < 0.01$ versus 3T3-L1 controls.

	3T3-L1 controls	3T3-L1/Mph co-cultured non-separated	3T3-L1/C2C12 co-cultured non-separated	3T3-L1/Mph co-cultured separated
	%	%	%	%
Phagocytic activity	22 ± 7	$45 \pm 5^*$	20 ± 5	26 ± 5
F4/80	0	$8.3 \pm 0.3^{**}$	0	0
Mac-1	0	$9 \pm 1^{**}$	0	0

responses (29, 30). However, after injection, the labeling of host cells caused by viral particles attached to the membrane of infected cells cannot be excluded. For all these reasons, CMV-GFP adenovirus was only used to check that our results were independent of the labeling technique.

After injection into the peritoneal cavity, most of the SVF cells as well as 3T3-L1 preadipocytes were very rapidly converted into cells which displayed the functional (high phagocytic capacity) and antigenic properties (expression of F4/80, Mac-1, and CD45) of neighboring peritoneal macrophages. This strongly argues for a phenotypic conversion of preadipocytes into typical macrophages. To complete this phenotype, the expression of proteins associated with antigen-presenting function was compared with that of peritoneal macrophages. Once again, CD80 and CD86 antibodies stained similar percentages of DAPI⁺ and peritoneal exudated cells. The peritoneal cavity of mouse can educate preadipocytes into phagocytosing cell that express the immunologically significant costimulation molecules B7.1 and B7.2 (CD80 and CD86).

The effect of peritoneal cavity on the preadipocyte phenotype is consistent with numerous studies on cellular plasticity in which the environmental and pathological context strongly direct the fate of injected cells whatever their tissue origins (31–33). An intriguing point is that differentiated cells present in the cavity, *i.e.* peritoneal macrophages, can induce the phenotypic transformation of precursor cells into their own phenotype. Although this conversion is very low *in vitro*, it is specific because no F4/80 or Mac-1 staining was detected when coculture was performed with the C2C12 myoblastic cell line. Very recently, it was shown that endothelial cells cultivated with cardiomyocytes could differentiate into cardiomyocytes (33). This suggests that differentiated cells are themselves strong inducers of their own differentiation program. In our study, direct contact between preadipocytes and macrophages seems to be required to achieve this phenotypic conversion, as demonstrated by the experiments using track-etched membrane separation. The involvement of cell-to-cell contact is not very surprising and underlines its role in many differentiation processes (34, 35). The nature of the observed phenotype change is very difficult to define precisely. It in fact corresponds to a conversion process between two lineages that were previously thought to be independent. Although it has been shown that preadipocyte cell lines could be induced to differentiate into other cell types, such as osteoblasts (36), the rapid kinetics of change could suggest a transdifferentiation process or/and a stronger lineage relationship between adipocyte progenitors and macrophages than expected.

Our study demonstrates that adipose progenitors can rapidly and efficiently convert into typical macrophages. This raises the possibility that the preadipocyte could have been changed into a cell capable of costimulating a T cell. Such interaction may influence the biology of both cell types and have grave implications in immunologic as well as metabolic pathogenic states. Increasing cross-talk between both fields are reported and emphasize the importance of inflammation in various metabolic disorders as diabetes, atherosclerosis, and obesity (16, 37–42). Overall, this underlines the plasticity of adipose precursor cells and reinforces the developing relationship between innate immunity and adipose tissue.

Acknowledgments—We thank C. Dani for helpful discussions. Adenovirus CMV-CFP was donated by the Association Française contre les Myopathies.

REFERENCES

- Hahn, P., and Novak, M. (1975) *J. Lipid Res.* **16**, 79–91
- Tisdale, M. J. (1997) *J. Natl. Cancer Inst.* **89**, 1763–1773
- Ailhaud, G., Grimaldi, P., and Negrel, R. (1992) *Annu. Rev. Nutr.* **12**, 207–233
- Zhang, B., Berger, J., Hu, E., Szalkowski, D., White-Carrington, S., Spiegelman, B. M., and Moller, D. E. (1996) *Mol. Endocrinol.* **10**, 1457–1466
- Ron, D., Brasier, A. R., McGehee, R. E., Jr., and Habener, J. F. (1992) *J. Clin. Invest.* **89**, 223–233
- Negrel, R., Grimaldi, P., Forest, C., and Ailhaud, G. (1985) *Methods Enzymol.* **109**, 377–385
- Takemura, R., and Werb, Z. (1984) *Am. J. Physiol.* **246**, C1–9
- Krieger-Brauer, H. I., and Kather, H. (1992) *J. Clin. Invest.* **89**, 1006–1013
- Scott, L. M., Civin, C. I., Rorth, P., and Friedman, A. D. (1992) *Blood* **80**, 1725–1735
- Tanaka, T., Yoshida, N., Kishimoto, T., and Akira, S. (1997) *EMBO J.* **16**, 7432–7443
- Ricote, M., Li, A. C., Willson, T. M., Kelly, C. J., and Glass, C. K. (1998) *Nature* **391**, 79–82
- Pelton, P. D., Zhou, L., Demarest, K. T., and Burris, T. P. (1999) *Biochem. Biophys. Res. Commun.* **261**, 456–458
- Aitman, T. J., Glazier, A. M., Wallace, C. A., Cooper, L. D., Norsworthy, P. J., Wahid, F. N., Al-Majali, K. M., Trembling, P. M., Mann, C. J., Shoulders, C. C., Graf, D., St Lezin, E., Kurtz, T. W., Kren, V., Pravenec, M., Ibrahim, A., Abumrad, N. A., Stanton, L. W., and Scott, J. (1999) *Nat. Genet.* **21**, 76–83
- Lin, Y., Lee, H., Berg, A. H., Lisanti, M. P., Shapiro, L., and Scherer, P. E. (2000) *J. Biol. Chem.* **275**, 24255–24263
- Cousin, B., Munoz, O., Andre, M., Fontanilles, A. M., Dani, C., Cousin, J. L., Laharrague, P., Casteilla, L., and Penicaud, L. (1999) *FASEB J.* **13**, 305–312
- Cousin, B., Andre, M., Casteilla, L., and Penicaud, L. (2001) *J. Cell. Physiol.* **186**, 380–386
- Martinez-Pomares, L., Platt, N., McKnight, A. J., da Silva, R. P., and Gordon, S. (1996) *Immunobiology* **195**, 407–416
- Soukas, A., Succi, N. D., Saatkamp, B. D., Novelli, S., and Friedman, J. M. (2001) *J. Biol. Chem.* **276**, 34167–34174
- Gerhold, D. L., Liu, F., Jiang, G., Li, Z., Xu, J., Lu, M., Sachs, J. R., Bagchi, A., Fridman, A., Holder, D. J., Doebber, T. W., Berger, J., Elbrecht, A., Moller, D. E., and Zhang, B. B. (2002) *Endocrinology* **143**, 2106–2118
- Alon, U., Barkai, N., Notterman, D. A., Gish, K., Ybarra, S., Mack, D., and Levine, A. J. (1999) *Proc. Natl. Acad. Sci. U. S. A.* **96**, 6745–6750
- Jiang, Y., Vaessen, B., Lenvik, T., Blackstad, M., Reyes, M., and Verfaillie, C. M. (2002) *Exp. Hematol.* **30**, 896–904
- Bjornorp, P., Karlsson, M., Pertoft, H., Pettersson, P., Sjostrom, L., and Smith, U. (1978) *J. Lipid Res.* **19**, 316–324
- Takao, S., Smith, E. H., Wang, D., Chan, C. K., Bulkley, G. B., and Klein, A. S. (1996) *Am. J. Physiol.* **271**, C1278–84
- Chomczynski, P., and Sacchi, N. (1987) *Anal. Biochem.* **162**, 156–159
- Dysvik, B., and Jonassen, I. (2001) *Bioinformatics* **17**, 369–370
- Dorfman, J., Duong, M., Zibaitis, A., Pelletier, M. P., Shum-Tim, D., Li, C., and Chiu, R. C. (1998) *J. Thorac. Cardiovasc. Surg.* **116**, 744–751
- Pye, D., and Watt, D. J. (2001) *J. Anat.* **198**, 163–173
- de Martin, R., Raidl, M., Hofer, E., and Binder, B. R. (1997) *Gene Ther.* **4**, 493–495
- Yang, Y., Li, Q., Ertl, H. C., and Wilson, J. M. (1995) *J. Virol.* **69**, 2004–2015
- Tripathy, S. K., Black, H. B., Goldwasser, E., and Leiden, J. M. (1996) *Nat. Med.* **2**, 545–550
- Ferrari, G., Cusella-De Angelis, G., Coletta, M., Paolucci, E., Stornaiuolo, A., Cossu, G., and Mavilio, F. (1998) *Science* **279**, 1528–1530
- Galli, R., Borello, U., Gritti, A., Minasi, M. G., Bjornson, C., Coletta, M., Mora, M., De Angelis, M. G., Fiocco, R., Cossu, G., and Vescovi, A. L. (2000) *Nat. Neurosci.* **3**, 986–991
- Condorelli, G., Borello, U., De Angelis, L., Latronico, M., Sirabella, D., Coletta, M., Galli, R., Balconi, G., Follenzi, A., Frati, G., Cusella De Angelis, M. G., Gioglio, L., Amuchastegui, S., Adorini, L., Naldini, L., Vescovi, A., Dejana, E., and Cossu, G. (2001) *Proc. Natl. Acad. Sci. U. S. A.* **98**, 10733–10738
- Prosper, F., and Verfaillie, C. M. (2001) *J. Leukoc. Biol.* **69**, 307–316
- Albelda, S. M., and Buck, C. A. (1990) *FASEB J.* **4**, 2868–2880
- Ji, X., Chen, D., Xu, C., Harris, S. E., Mundy, G. R., and Yoneda, T. (2000) *J. Bone Miner. Metab.* **18**, 132–139
- Marti, A., Marcos, A., and Martinez, J. A. (2001) *Obes. Rev.* **2**, 131–140
- Hansson, G. K., Libby, P., Schonbeck, U., and Yan, Z. Q. (2002) *Circ. Res.* **91**, 281–291
- Daynes, R. A., and Jones, D. C. (2002) *Nat. Rev. Immunol.* **2**, 748–759
- Wilkin, T. J. (2001) *Diabetologia* **44**, 914–922
- Barbier, O., Torra, I. P., Duguay, Y., Blanquart, C., Fruchart, J. C., Glineur, C., and Staels, B. (2002) *Arterioscler. Thromb. Vasc. Biol.* **22**, 717–726
- Natarajan, C., and Bright, J. J. (2002) *Genes Immun.* **3**, 59–70

Preadipocyte Conversion to Macrophage: EVIDENCE OF PLASTICITY
Guillaume Charrière, Béatrice Cousin, Emmanuelle Arnaud, Mireille André, Francis
Bacou, Luc Pénicaud and Louis Casteilla

J. Biol. Chem. 2003, 278:9850-9855.

doi: 10.1074/jbc.M210811200 originally published online January 7, 2003

Access the most updated version of this article at doi: [10.1074/jbc.M210811200](https://doi.org/10.1074/jbc.M210811200)

Alerts:

- [When this article is cited](#)
- [When a correction for this article is posted](#)

[Click here](#) to choose from all of JBC's e-mail alerts

This article cites 42 references, 16 of which can be accessed free at
<http://www.jbc.org/content/278/11/9850.full.html#ref-list-1>